Colonization and bioweathering of monazite by Aspergillus niger

Kang, Xia; Csetenyi, Laszlo; Gadd, Geoffrey Michael

Published in:
Environmental Microbiology

DOI:
10.1111/1462-2920.15402

Publication date:
2021

environmental microbiology

Environmental Microbiology (2021) **23**(7), 3970–3986 doi:10.1111/1462-2920.15402

Special Issue Article

Colonization and bioweathering of monazite by *Aspergillus niger*: solubilization and precipitation of rare earth elements

Xia Kang,[1] Laszlo Csetenyi[2] and Geoffrey Michael Gadd [1,3]*

[1]*Geomicrobiology Group, School of Life Sciences, University of Dundee, Dundee, Scotland, DD1 5EH, UK.*

[2]*Concrete Technology Group, Department of Civil Engineering, University of Dundee, Dundee, Scotland, DD1 4HN, UK.*

[3]*State Key Laboratory of Heavy Oil Processing, Beijing Key Laboratory of Oil and Gas Pollution Control, College of Chemical Engineering and Environment, China University of Petroleum, 18 Fuxue Road, Changping District, Beijing, 102249, China.*

Summary

Geoactive fungi play a significant role in bioweathering of rock and mineral substrates. Monazite is a phosphate mineral containing the rare earth elements (REE) cerium, lanthanum and neodymium. Little is known about geomicrobial transformations of REE-bearing minerals which are also relevant to REE biorecovery from terrestrial and extra-terrestrial reserves. The geoactive soil fungus *Aspergillus niger* colonized monazite in solid and liquid growth media without any apparent growth inhibition. In a glucose-minerals salts medium, monazite enhanced growth and mycelium extensively covered rock particle surfaces, probably due to the provision of phosphate and essential trace metals. Teeth-like and pagoda-like etching patterns indicated monazite dissolution, with extensive precipitation of secondary oxalate minerals. Biomechanical forces ensued causing aggressive bioweathering effects by tunnelling, penetration and splitting of the ore particles. High amounts of oxalic acid (~46 mM) and moderate amounts of citric acid (~5 mM) were produced in liquid media containing 2% (wt./vol.) monazite, and REE and phosphate were released. Correlation analysis suggested that citric acid was more effective than oxalic acid in REE mobilization, although the higher concentration of oxalic acid also implied complexant activity, as well as the prime role in REE-oxalate precipitation.

Received 2 December, 2020; revised 14 January, 2021; accepted 15 January, 2021. *For correspondence. E-mail g.m.gadd@dundee.ac.uk; Tel. +44 1382 384767.

Introduction

The activities of living organisms can lead to degradation, deterioration, erosion and weathering of both natural and synthetic materials (Mottershead *et al*., 2003; Gadd, 2010, 2017a; Ma *et al*., 2020). Fungal-induced rock and mineral bioweathering plays an important part in the lithological biogeochemical cycling of carbon, phosphorus and essential metal elements such as K, Ca and Mg (Hoffland *et al*., 2004). Common rock types such as granite, limestone, marble and sandstone are prone to colonization, biodeterioration and bioweathering by a wide range of lichenized, free-living, and microcolonial fungi, and bacteria (Staley *et al*., 1982; Wollenzien *et al*., 1995; Burford *et al*., 2003a, 2003b; Gadd, 2017a). Moreover, many mineral- and rock-based structures can support a diverse array of 'rock-eating' fungi, which play a key role in mineral diagenesis and pedogenesis of the terrestrial ecosystem (Gleeson *et al*., 2005; van Schöll *et al*., 2008).

Microorganisms inflict bioweathering on minerals and rocks mainly in two ways, i.e. biochemical and biomechanical mechanisms (Gadd, 2010, 2017b). Biochemical weathering involves precipitation, complexation, chelation and redox reactions mediated by a range of substances, e.g. low-molecular-weight organic-acids (LMWOAs), siderophores, extracellular polymeric substances and exoenzymes excreted by fungi (Hirsch *et al*., 1995; Uroz *et al*., 2009; Kirtzel *et al*., 2020). Since organic acids produced by fungi exhibit remarkable abilities to solubilize and transform minerals, they have received wide attention in research on fungi–mineral interactions (Bolan *et al*., 1994; Gadd, 1999). Carbonates (e.g. dolomite),

oxides (e.g. laterite), phosphates (e.g. apatite) and silicates (e.g. biotite) can all be affected by organic acids resulting in etching, deterioration and alteration of rock surfaces (de la Torre *et al*., 1992; Adeyemi and Gadd, 2005; Ceci *et al*., 2015b; Yang *et al*., 2019). One classical example is the solubilization of apatite [$Ca_5(PO_4)_3$] by ectomycorrhizal fungi, leading to the mobilization of calcium and phosphate which can promote soil fertility (Whitelaw *et al*., 1999; Landeweert *et al*., 2001; Hoffland *et al*., 2004). Biomechanical effects include physical forces exerted by the filamentous hyphae during cryptoendolithic proliferation and biofouling of the rock substrate (Fomina *et al*., 2010; Gadd, 2017c; Mergelov *et al*., 2018). Cavities, cracks and fissures can provide an ideal microenvironment for rock-dwelling microbial communities (Gadd, 2007; Wei *et al*., 2012). Fungi exhibit excellent capabilities in colonizing such habitats by means of hyphal boring, tunnelling and penetration (Fuhr *et al*., 2013; Ceci *et al*., 2015a; Ferrier *et al*., 2019). With a combination of these two, often synergistic, mechanisms, fungi have a huge impact on the Earth's lithosphere and pedosphere (Burford *et al*., 2003b).

Although the sustainability of metal mining with depletion of natural Earth resources has been questioned for many years (Skinner, 1979), it is only in recent years that such an issue has engendered worldwide concern, particularly with the growth of advanced electronic and digital technologies that require ever-increasing amounts of a wide range of valuable elements (Graedel *et al*., 2015; Liang and Gadd, 2017; Wall *et al*., 2017). Rare earth elements (REE) are particularly important among the so-called critical or E-tech elements and their security of supply is threatened by depletion of natural sources, inadequate reclamation and recycling, and geopolitical threats (Humphries, 2012; Massari and Ruberti, 2013; Barmettler *et al*., 2016; Goodenough *et al*., 2016; Wall *et al*., 2017). With the development of new technologies to address this problem, bioprocessing is viewed as a promising adjunct or alternative to conventional techniques, with a long history of success in the bioleaching industry (Johnson, 2014, 2018). Nevertheless, new sources of critical elements need to be found with deep-sea sediments, reserves and manganese nodules all receiving growing attention (Hein *et al*., 2013; Hein, 2016; Kuhn *et al*., 2017; Ferrier *et al*., 2019). Furthermore, there is increasing interest in extra-terrestrial sources of metals and minerals and their harvest. Asteroids, meteorites and planets can contain significant amounts of valuable elements, including REE (McLeod and Krekeler, 2017; Anderson *et al*., 2019), and it has been shown that metal-transforming microorganisms can function under conditions of zero- and Mars gravity providing speculation about *in situ* metal bioprocessing in space vehicles and structures (Cockell *et al*., 2020). It is therefore important to fully understand the kinds of microbial processes that may be involved in metal–mineral interactions with such substrates which may inform methods for extraction, transformation or biorecovery, as well as extending knowledge about the geomicrobiology of rare but important metal and mineral resources (Zhuang *et al*., 2015; Barmettler *et al*., 2016).

Monazite contains Ce, La and Nd and is a crucial industrial resource of such REE worldwide (Haque *et al*., 2014). It is also a phosphate mineral and contains various other elements in small amounts (Kang *et al*., 2020). Previous research showed that monazite can be transformed into REE-oxalates, exhibiting a variety of crystal morphologies during incubation with *Aspergillus niger*, which demonstrated direct fungal–monazite interactions (Kang *et al*., 2020). However, most applied studies have concentrated on bioleaching and element recovery from REE minerals from a purely practical perspective with little attention paid to the basic understanding of the direct interaction mechanisms between REE-containing substrates and interacting microorganisms. *Aspergillus niger* is both industrially important and geoactive (Bennett, 1998; Gadd, 2017a). It exhibits outstanding competence in the biotransformation of minerals including zinc silicate, apatite, pyromorphite [$Pb_5(PO_4)_3Cl$], gypsum and struvite ($MgNH_4PO_4{\cdot}6H_2O$) (Gharieb and Gadd, 1999; Wei *et al*., 2013; Ceci *et al*., 2015b; Liang *et al*., 2016; Mendes *et al*., 2020; Suyamud *et al*., 2020). In addition, *A. niger* can corrode and transform copper metal through the excretion of oxalic acid (Zhao *et al*., 2020). Therefore, it is hypothesized that *A. niger* may directly interact with monazite through similar mechanisms.

The objective of this research was to examine the direct influence of *A. niger* on the weathering of Gakara monazite and to explore the mechanisms that are involved. By dissecting the intimate relationships between filamentous fungi and high-grade REE ores, this work will not only provide fundamental scientific knowledge but also indicate the potential for future prospects in the microbial processing of rare earth minerals with recycling, biohydrometallurgical and biomining implications.

Results

Monazite colonization, etching and bioweathering

Light microscopy showed that after 2 weeks of incubation with *A. niger* on Modified Czapek-Dox (MCD) plates in the dark at 25 °C, proliferation of mycelia appeared as yellow-coloured halos surrounding the monazite rock particles and this was more obvious with increasing

incubation time (see yellow arrows in Fig. 1A–D). Light microscopy showed that the particles recovered from MCD plates after 4 and 5 weeks of incubation were completely covered by *A. niger* mycelia. Compared with monazite rock particles in MCD media, no obvious halos were found around those in MEA media after 5 weeks of incubation with *A. niger* (Fig. 1G).

Scanning electron microscopy (SEM) revealed that after 2 weeks of incubation with *A. niger* on MCD plates, monazite rock particles were fully colonized with mycelia and exhibited a coarse surface texture (Fig. 2). Crystals of secondary minerals were formed individually and in clusters on the surface of the monazite rock particles (yellow arrows in Fig. 2B and F). Each individual crystal showed a layered morphology as it grew larger. These crystals were of various sizes from ~10 to 50 μm in length and ~10 μm in width (Fig. 2F). Fungal hyphae were observed growing out of cavities on monazite surfaces (white arrow in Fig. 2B) and also penetrating into the substrate causing a dent on the rock particle surface (white arrow in Fig. 2C). Etching patterns of irregular shape were widely observed on the weathered monazite

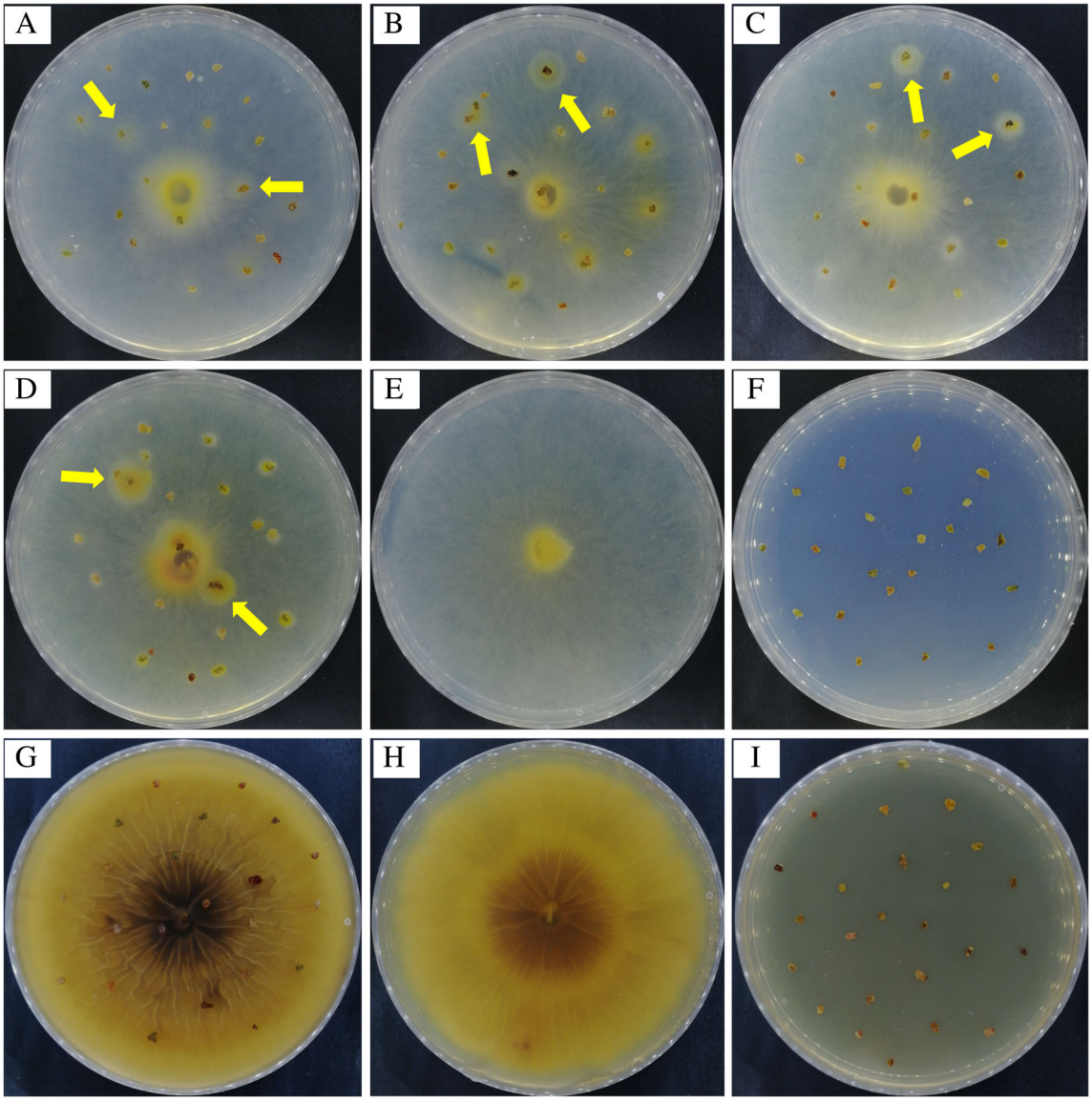

Fig 1. Colonization of monazite by *A. niger* after (A) 2, (B) 3, (C) 4 and (D) 5 weeks of incubation at 25 °C in the dark on MCD agar; (E) monazite-free MCD plate; (F) *A. niger*-free MCD plate. (G) Monazite rock particles in MEA plate after 5 weeks of incubation with *A. niger*; (H) monazite-free MEA plate; (I) *A. niger*-free MEA plate. Yellow arrows indicate halos of mycelia around monazite rock particles. Typical images are shown from many similar examinations. [Color figure can be viewed at wileyonlinelibrary.com]

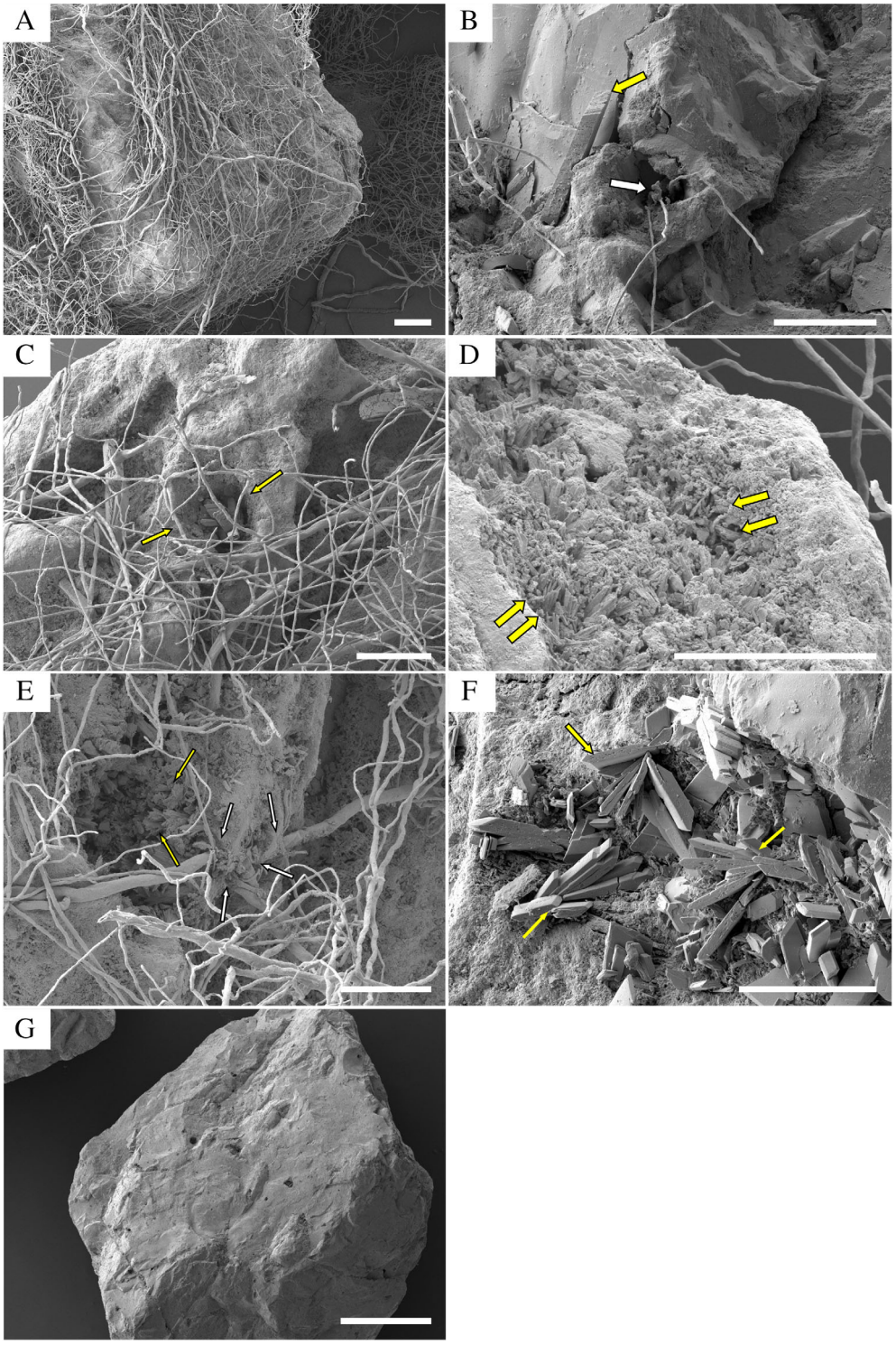

Fig 2. Scanning electron microscopy (SEM) of monazite rock particles after 2 weeks of incubation with *A. niger* on MCD plates at 25 °C in the dark.
(A) Colonized monazite rock particles covered by *A. niger* mycelia; (B) white arrow shows euendolithic growth of hyphae in a cavity, the yellow arrow indicates a secondary crystal; (C) yellow arrows indicate a depression in the monazite surface; (D) yellow arrows indicate etching patterns on the monazite surface; (E) white arrows indicate penetration of hyphae into the monazite, yellow arrows indicate etching patterns; (F) yellow arrows indicate secondary crystals.
(G) An untreated Gakara monazite rock particle. Scale bars = 500 μm. Scale bars: (A) 100 μm, (B–F) 50 μm, (G) 500 μm. Typical images are shown from many similar examinations. [Color figure can be viewed at wileyonlinelibrary.com]

surface (yellow arrows in Fig. 2D–E) and hyphae were observed penetrating through the etched substrate (white arrows in Fig. 2E). In contrast, the untreated monazite rock particles possessed a smooth surface (Fig. 2G). After 4 and 5 weeks of incubation, most mature crystals became detached from the more rugged monazite surface as bioweathering exacerbated. The attack of monazite by *A*. *niger* mycelia proceeded at a larger scale with time and large grooves resulted from hyphae colonizing the etched surface and penetrating through crevices (yellow arrows in Fig. 3B–F). However, throughout 5 weeks of incubation of *A*. *niger* on MEA plates, neither crystal formation nor etchings were observed on the monazite surface, which was only partially colonized by the mycelia (Fig. 4). SEM showed that after 2 weeks of incubation with *A*. *niger* in liquid MCD medium, secondary biominerals of a prismatic morphology and measuring ~10–20 μm in length emerged on the surface of the monazite grains (Fig. 5A). After 4 weeks of incubation, more secondary crystals were formed in aggregates with a more pronounced crystalline structure and of varying sizes (Fig. 5B). Yarn-like etching structures with a criss-cross pattern were observed on the surface of monazite after 2 weeks of incubation (Fig. 5C). The etching pattern on monazite was very obvious and appeared to have a rough and jagged texture (Fig. 5D). A large amount of

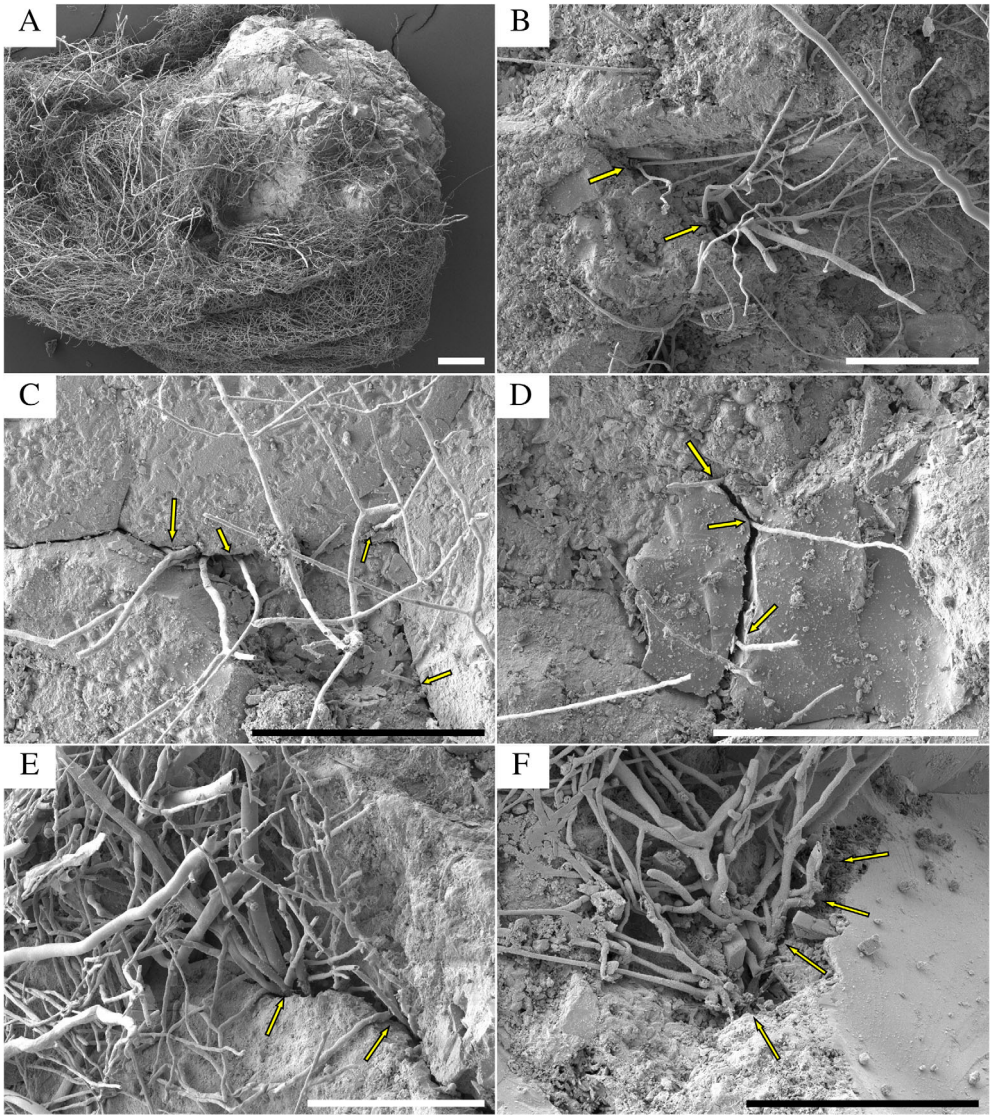

Fig 3. Scanning electron microscopy (SEM) of monazite rock particles after (A–D) 4 and (E–F) 5 weeks of incubation with *A*. *niger* on MCD plates at 25 °C in the dark.
(A) Colonized monazite rock particles covered by *A*. *niger* mycelia; (B) yellow arrows show euendolithic growth of hyphae in a cavity; (C–F) yellow arrows indicate chasmoendolithic growth of hyphae into fissures in monazite rock particles. Scale bars: (A) 200 μm, (B–F) 100 μm. Typical images are shown from many similar examinations. [Color figure can be viewed at wileyonlinelibrary.com]

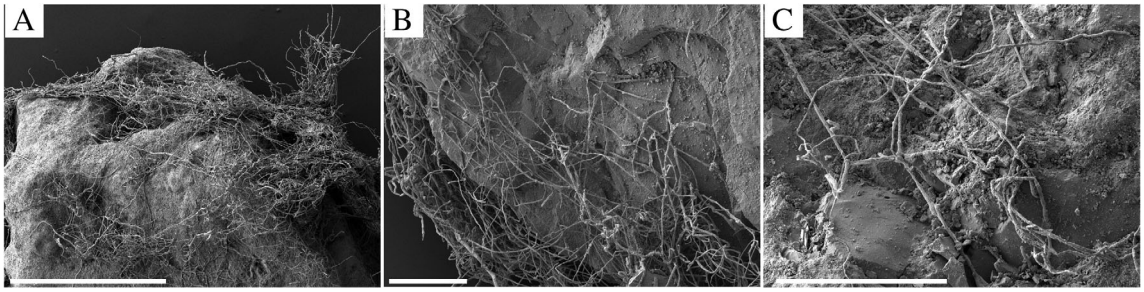

Fig 4. Scanning electron microscopy (SEM) of the monazite rock particles after 5 weeks of incubation with *A. niger* in MEA agar at 25 °C in the dark. Scale bars: (A) 500 μm, (B and C) 100 μm. Typical images are shown from many similar examinations.

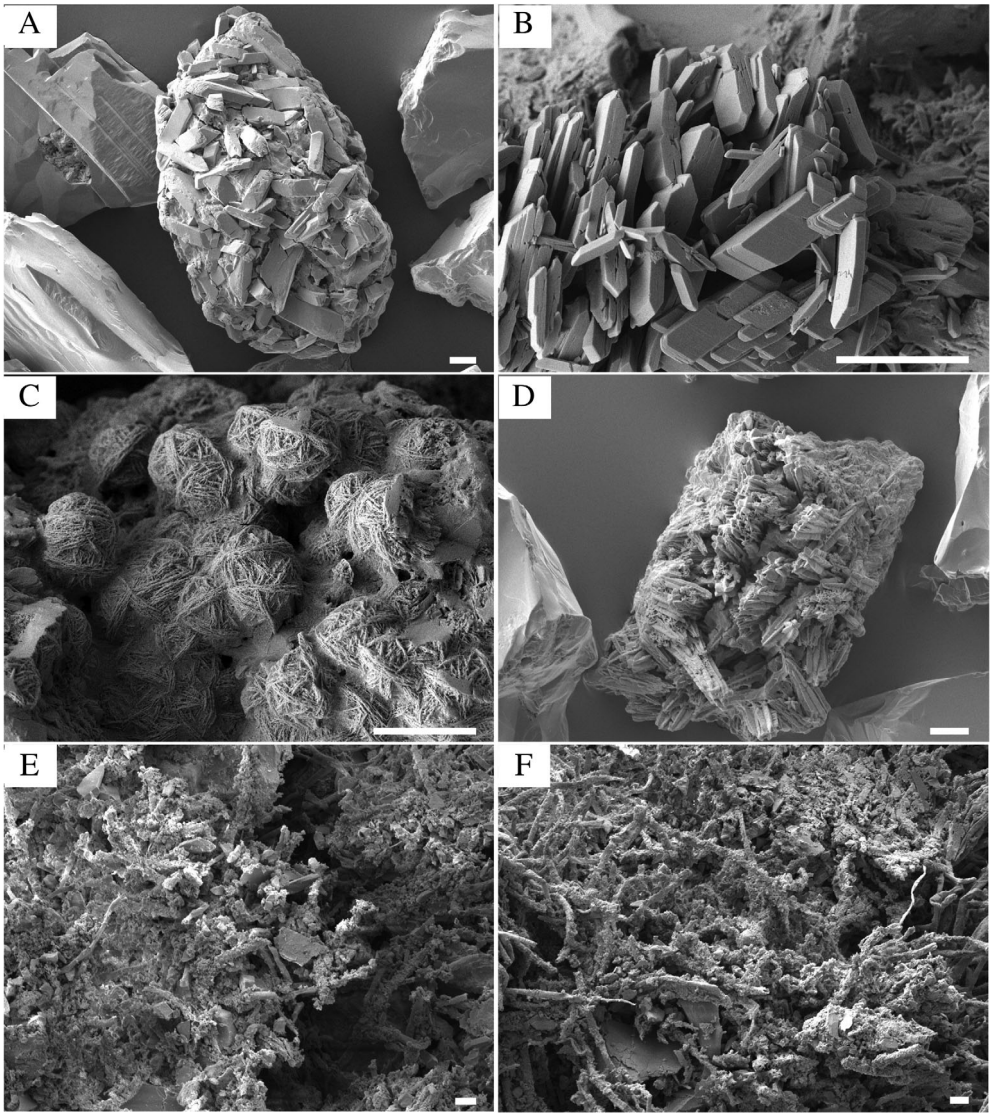

Fig 5. Scanning electron microscopy (SEM) of direct interactions between monazite and *A. niger* in liquid MCD medium supplemented with 2% monazite after (A, C and E) 2 and (B, D and F) 4 weeks of shake incubation with *A. niger* at 25 °C in the dark.
(A–B) Secondary crystals forming on the surface of a monazite grain; (C–D) etching patterns on the surface of monazite grains; (E and F) monazite-associated mycelia inside a fungal pellet. Scale bars = 10 μm. Typical images are shown from many similar examinations.

monazite debris was observed to be associated with mycelia inside the *A. niger* pellets after 2 and 4 weeks of incubation (Fig. 5E and F).

Energy-dispersive X-ray analysis (EDXA) showed that the secondary crystals produced on MCD agar plates were composed of high amounts of Ce, followed by La and a small amount of Nd (Fig. 6B). The etching patterns and untreated monazite also comprised Ce, La and Nd, the only difference being the presence of P and a lower C:O ratio compared with the secondary crystals (Fig. 6A and C). EDXA of the samples from liquid MCD medium revealed that the secondary crystals, though consisting of Ce, La and Nd, were devoid of P (Fig. 6D), whereas the etching pattern invariably consisted of a similar elemental composition as the untreated sample, which featured high peaks for P and a small amount of Ca (Fig. 6E).

Organic acid production, REE and inorganic phosphate (P_i) release, and medium pH changes

The oxalic acid concentration in monazite-containing MCD medium after 2 weeks of incubation significantly increased ($P < 0.05$) compared with the first week to a peak of 46.23 ± 1.19 mM, after which a slightly declining trend followed to 41.39 ± 5.41 mM in the final week (Fig. 7A). In MEA containing 2% (wt./vol.) monazite, oxalic acid concentrations were much lower, reaching 13.83 ± 0.33 mM after 5 weeks of incubation (data not shown). The oxalic acid concentration in monazite-free MCD medium showed a continuous increase over the 5 week incubation period, reaching 39.11 ± 9.78 mM in the final week. Oxalic acid concentrations in all the test samples were significantly higher than in the control groups after 1 ($P < 0.05$), 2 ($P < 0.01$), 3 ($P < 0.05$) and

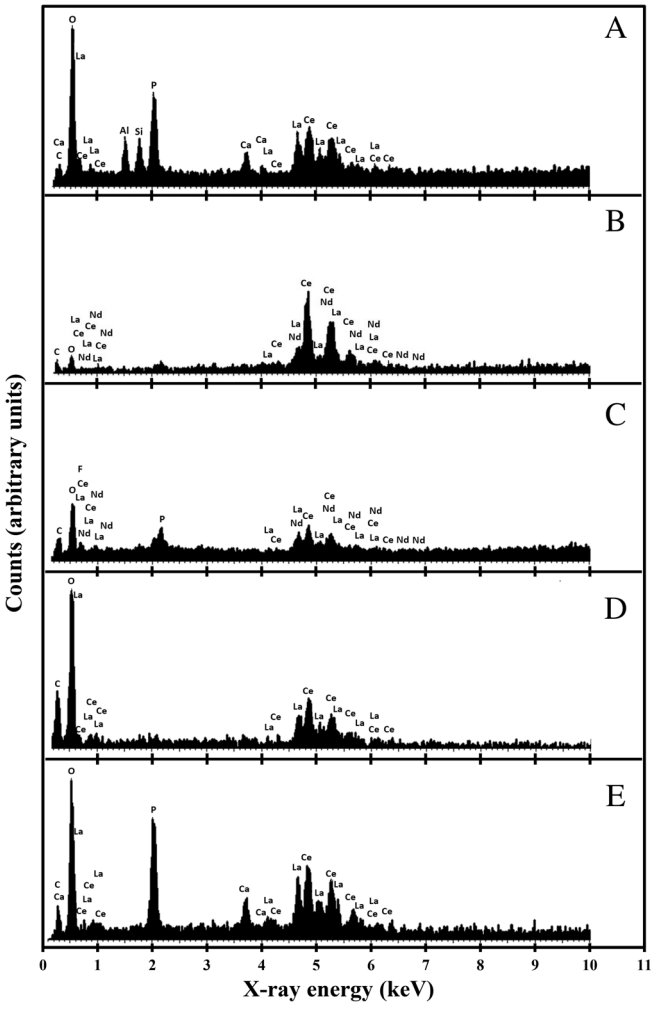

Fig 6. (A) Energy-dispersive X-ray analysis (EDXA) of the untreated monazite sample; EDXA of (B) secondary crystals and (C) the etching patterns on monazite grains after 5 weeks of incubation with *A. niger* in MCD agar; EDXA of (D) secondary crystals and (E) the etching patterns on monazite grains after shake incubation of *A. niger* with 2% (wt./vol.) monazite in liquid MCD medium at 25 °C in the dark. Typical spectra are shown from several similar determinations.

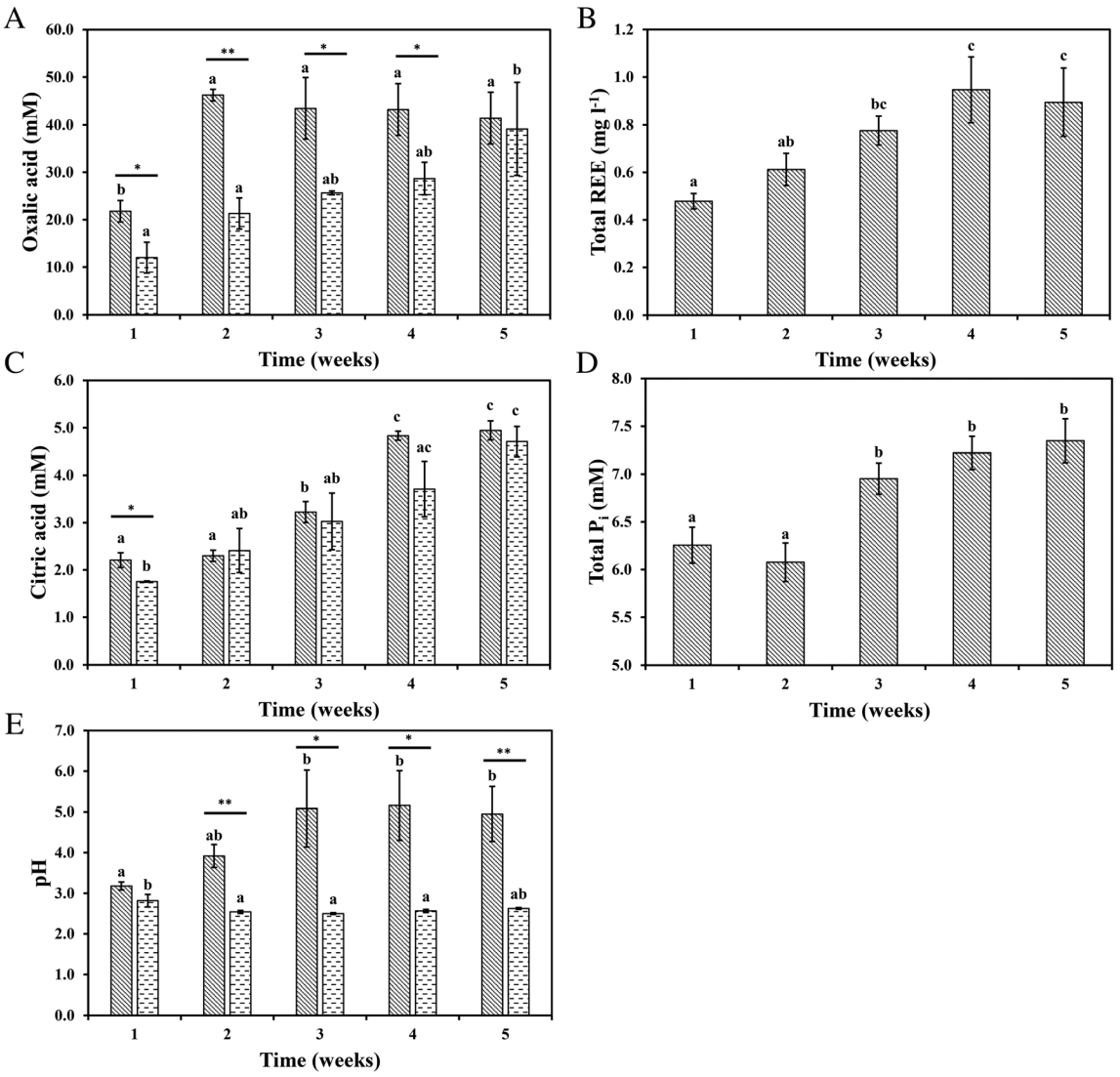

Fig 7. Bar charts of (A) oxalic acid concentration, (B) citric acid concentration, (C) pH, (D) total REE concentration and (E) total soluble P_i concentration in liquid MCD media over 5 weeks of shake incubation at 25 °C in the dark. (▨) Liquid MCD medium containing 2% (wt./vol.) monazite; (▨) monazite-free liquid MCD medium. Data are averages of at least three replicates and error bars show the standard error of the mean. Different lowercase letters among each treatment indicate significant differences ($P < 0.05$) for different weeks based on Tukey's test. The difference between two treatments for each week is flagged with two stars (**) at $0.001 < P < 0.01$ and one star (*) at $0.01 < P < 0.05$ based on Student's *t*-test.

4 ($P < 0.05$) weeks of incubation although values were very close in the final week. Citric acid was also detected in liquid MCD medium. Citric acid was not detected in MEA. The amount of citric acid in monazite-containing MCD medium significantly increased ($P < 0.05$) to 3.22 ± 0.22 mM after 3 weeks of incubation and finally reached 4.94 ± 0.20 mM (Fig. 7C). Slightly more citric acid was produced in the test than in the monazite-free control groups after 3, 4 and 5 weeks of incubation but this was not statistically significant. Total REE concentrations in the supernatant showed an increasing trend ranging between 0.4 and 1.1 mg L^{-1} in MCD medium and reaching a plateau after 4 weeks of incubation (Fig. 7B). The total soluble P_i concentration in monazite-containing MCD media significantly increased to 6.95 ± 0.16 mM ($P < 0.05$) after 3 weeks of incubation and reached 7.35 ± 0.23 mM in the final week (Fig. 7D). Note that total P concentrations in monazite-free MCD and MEA media were 7.0 and 0.47 mM respectively. In liquid MCD medium containing 2% (wt./vol.) monazite, the pH showed an increasing trend from ~pH 3 to 6, while in the monazite-free control the value was slightly

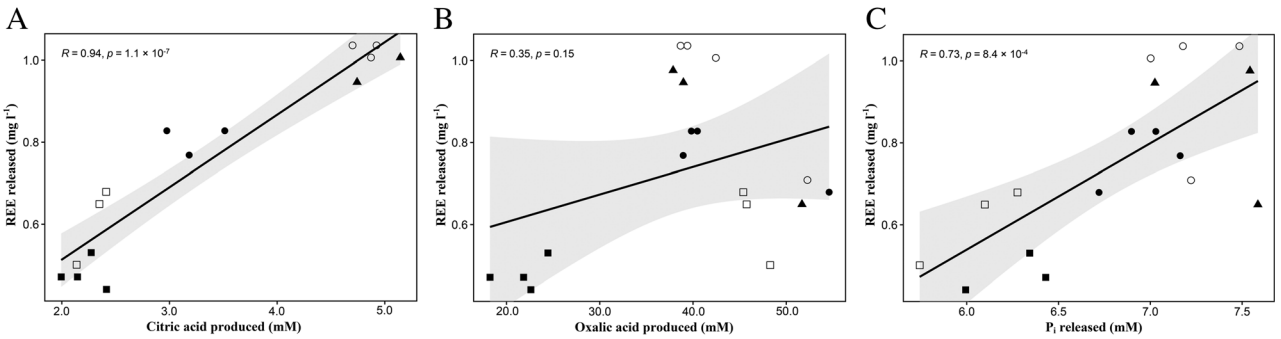

Fig 8. Pearson correlation analysis of (A) citric acid production versus REE release, (B) oxalic acid production versus REE release, and (C) the dissociation of REE-phosphates in liquid MCD medium supplemented with 2% monazite and inoculated with *A. niger* over (■) 1, (□) 2, (●) 3, (○) 4 and (▲) 5 weeks of shake incubation at 25 °C in the dark. *R*-value indicates Pearson's correlation coefficient; *P*-value indicates significance; the grey area around the linear trend line represents the confidence interval.

lower only in the third week (Fig. 7E). Comparisons between the two treatments showed that, from the second week onwards, the pH in MCD medium containing 2% monazite was always significantly higher than the control ($P < 0.05$), the latter being between pH 2.5 and 2.9 during the entire incubation period.

Correlation analysis

Pearson correlation analysis was performed to investigate the pairwise relationship between acid production, P_i and REE release. In liquid MCD medium, a significance correlation ($P = 1.1 \times 10^{-7}$) was found between citric acid and REE concentrations with a very strong degree of association at $R = 0.94$ (Fig. 8A). The correlation between oxalic acid and REE concentrations was positive but weak at Pearson's $R = 0.35$ without statistical significance ($P = 0.15$) (Fig. 8B). The association between the concentrations of P_i and REE in the medium was also found to be strong at $R = 0.94$ and statistically significant ($P = 8.4 \times 10^{-4}$) (Fig. 8C).

Discussion

Because of the worldwide concern over the security of supply of critical elements that power the modern age, novel bioprocessing approaches for their extraction and biorecovery are receiving growing interest (Zhuang *et al*., 2015; Barmettler *et al*., 2016; Liang and Gadd, 2017). Apart from improved reclamation and recycling from low-grade ores and mining residues, process streams and electronic wastes, deep oceanic reserves and extra-terrestrial sources are also receiving growing attention. Asteroids and other celestial bodies are replete with important metals and minerals and viewed as a future ambitious option for element recovery (McLeod and Krekeler, 2017; Anderson *et al*., 2019; Cockell *et al*., 2020). It is also relevant that there is a relative dearth of information about the geomicrobiology of the rarer elements and it is therefore important to understand the mechanisms by which organisms may interact with and transform such metal-bearing substrates. Fungi are capable of effecting many metal and mineral transformations, underpinned by their filamentous growth form and chemoorganotrophic metabolism, which are of major biogeochemical importance in terrestrial and aquatic habitats (Gadd, 2007, 2017a). Many can grow under so-called extreme environmental conditions and exhibit marked tolerance to potentially toxic metals and investigations of their interactions with metal-bearing Earth minerals is therefore relevant to both geomicrobiology and environmental biotechnology (Gadd, 2007, 2010). In this research, we have investigated fungal interactions with monazite sand, a rare phosphate mineral (formula: Ce, La, Nd, Th)(PO_4, SiO_4) and an important industrial source of REE. Conventional processing is energy-intensive and may involve sulfuric acid leaching at high temperature, various filtration, solvent extraction, and neutralization steps and/or precipitation of REE by oxalate (Kumari *et al*., 2015). Many fungi are capable of metal immobilization as oxalates mediated by high oxalic acid excretion (Fomina *et al*., 2005b; Gadd *et al*., 2014), providing further rationale and relevance for this investigation.

The rapid colonization of monazite by *A. niger* mycelia in solid MCD medium suggested that the fungus was not inhibited by the REE released which could pose a potential threat to the organisms. The expanding halos around the monazite particles were indicative of mycelial overgrowth, which was further revealed by examination of harvested monazite rock particles which showed mycelia tightly attached to the surface. SEM also confirmed that the rock particles in MEA agar were only loosely associated with hyphae after 5 weeks of incubation compared with those in MCD plates. It is interesting to note that *A. niger* grown in MEA plates, although growing more

luxuriantly than on MCD plates, did not show such biomass proliferation around the rock particles. This could be due to the nutrient composition of the different growth media. Undefined growth media such as MEA (containing malt extract and peptone) and potato dextrose agar, though rich in a variety of nutrients, are not designed for producing high amounts of organic acids in industrial fermentation processes (Paik *et al*., 1991; Jan *et al*., 1994; Padmavathi, 2015). Synthetic medium is commonly used for organic acid production, and the amount of secretion is mainly associated with the concentrations of carbon source (glucose or sucrose), nitrogen source (nitrate) and phosphorus (Aghaie *et al*., 2009; Amiri *et al*., 2012; Betiku *et al*., 2016; Bahaloo-Horeh and Mousavi, 2017; Faraji *et al*., 2018). This is in agreement with our research, where the amount of oxalic acid produced by *A*. *niger* in MCD medium was approximately 3.3× the amount produced in MEA medium. Furthermore, fungi may respond differently to the amount of phosphorus source. One study showed that citric acid production by *A*. *niger* was positively correlated with the concentration of phosphate in the medium (Upton *et al*., 2017). Another study showed that reducing the phosphate concentration increased solubilization of $Co_3(PO_4)_2$ but reduced solubilization of $Zn_3(PO_4)_2$ (Dixon-Hardy *et al*., 1998). Mineralogical analysis of the monazite used in this research showed that, in addition to Ce, La and Nd, the sample contained Mn (7.9% MnO), Fe (2.9% Fe_2O_3), Ca (1.0% CaO), Mg (0.44% MgO), all of which can serve as essential trace metals (Kang *et al*., 2020). Biogenic organic acids produced by *A*. *niger* can effectively facilitate the dissolution of phosphate minerals (Schneider *et al*., 2010; Gadd, 2017a), leading to the release of P_i and also trace metals from the monazite. Moreover, it was reported that ectomycorrhizal fungi were able to mobilize nutrients from insoluble sources such as calcite and soil mineral grains under nutrient-deficient conditions (Jongmans *et al*., 1997; van Schöll *et al*., 2008). Therefore, an explanation of the colonization with a marked increase in mycelial growth around the monazite rock particles could be due to the elevated oxalic acid production and the subsequent release of P_i and bioavailable trace metals in MCD medium.

The rugged surface of the monazite showed signs of bioweathering and mineral solubilization after 2 weeks colonization by *A*. *niger* in solid MCD medium, probably through biochemical mechanisms such as organic acid leaching which is a feature of many *Aspergillus* species (Hassanien *et al*., 2014). Solubilization of phosphates by acid-producing fungi has been reported in many studies (Jacobs *et al*., 2002a, 2002b; Fomina *et al*., 2004, 2005a, 2006; Sabre *et al*., 2009).

Etchings began to develop as soon as the monazite surface was covered with a mat of mycelia. EDXA confirmed that the etching patterns showed a similar elemental composition to the untreated monazite. Similar teeth-like etching patterns were observed when apatite (Ca phosphate) particles were incubated for 4 years in the rhizosphere of an old beech tree (Uroz *et al*., 2009). Depressions in the surface under hyphae and the irregular etching patterns suggested the chemical dissolution of the REE-phosphate substrate. Physical bioweathering attacks such as tunnelling and mechanical penetration commenced after the second week of incubation, which confirmed that the mycelia were actively colonizing the substrate. After prolonged incubation, many hyphal strands penetrated into the monazite particles through surface cavities and fissures. A similar phenomenon was observed for hyphae of *Schizophyllum commune* splitting off fragments during black slate colonization (Kirtzel *et al*., 2020). One study claimed that the hyphae of some 'rock-eating' mycorrhizal fungi were able to bore through rocks as hard as granite (Jongmans *et al*., 1997). Based on evidence from limestone colonization by *Penicillium corylophilum*, it was hypothesized that fungal hyphae can burrow into pre-existing cracks, fissures and weak points of the rock surface (Fomina *et al*., 2010), which provides more corroborating evidence for this study. The rock particles colonized by *A*. *niger* in MEA medium only showed a weathered surface without signs of hyphal tunnelling or penetration, which also implied that the fungus had less of a requirement to access nutrients contained in the monazite while already thriving in a nutrient-rich medium. In liquid culture, the etchings were more obvious and changed from yarn-like to more jagged structures which were probably due to the high concentrations of produced organic acids and physical contact with the mycelia. EDXA confirmed that the elemental composition of etched surfaces was similar to untreated monazite as indicated by the presence of P and a lower C:O ratio, although it is noted that EDXA may provide no information as to possible mineralogical changes in the substrate.

Secondary mineral crystals were observed on monazite surfaces most conspicuously after the second week of incubation when the rock particles had been completely colonized. The absence of P and a higher C:O ratio in the EDX spectrum suggested that the secondary minerals were REE-oxalates which were identified conclusively using XRD in previous research (Kang *et al*., 2019, 2020). Many studies have shown that oxalate production leads to the formation of secondary oxalate minerals which play a key role in the biodeterioration of carbonate rocks and metal-bearing minerals (Hirsch *et al*., 1995; Adeyemi and Gadd, 2005; Gadd *et al*., 2014; Sturm *et al*., 2015). The distinctive layered texture also indicated that they were gradually precipitated with the accretion of oxalate produced by the fungus. As oxalate

crystals grew larger, they could not fully adhere to the surface and began to shed. Such formation of secondary crystals occurred in conjunction with bioweathering effects throughout the whole incubation period of fungal growth. The formation of secondary minerals also occurred as clusters on the surface of monazite grains in liquid MCD culture, and abundant secondary crystals were formed as oxalic acid accumulated in the medium.

The low production of citric acid in MCD medium could be explained by the choice of carbon source, as it has been clarified that sucrose is the preferred carbon source for the production of citric acid by *A. niger* (Hossain *et al*., 1984). The significantly higher amounts of oxalic and citric acid in monazite-containing MCD medium compared with the control could be a result of two factors, i.e. the rise in pH and the release of inorganic phosphate. An increase in the pH of media can enhance the activity of oxalacetate acetylhydrolase (OAH), an essential enzyme required for the biosynthesis of oxalic acid in fungi, and OAH activity can double with a pH increase from pH 2.5 to 5 (Ruijter *et al*., 1999). Positive feedback may result from solubilized PO_4^{3-} acting as an effective buffer, accepting protons causing the balance to shift towards producing more organic acids (Strasser *et al*., 1994; Magnuson and Lasure, 2004; Brisson *et al*., 2016). Such a mechanism may be summarized in the following equations (Dickson and Riley, 1979; Jiang, 1996):

$$H_2C_2O_4 \rightleftharpoons C_2O_4^{2-} + 2H^+ \quad (1)$$

$$H^+ + PO_4^{3-} \rightleftharpoons HPO_4^{2-} \quad (2)$$

$$H^+ + HPO_4^{2-} \rightleftharpoons H_2PO_4^- \quad (3)$$

$$H^+ + H_2PO_4^- \rightleftharpoons H_3PO_4 \quad (4)$$

An increase of pH in the presence of 2% monazite in MCD medium was therefore caused by the buffering effect of soluble phosphate species, which were liberated through the solubilization of REE-phosphates in the monazite. Similar phenomena have also been observed in co-culture experiments with fungi and tellurite (Te^{IV}), tricalcium phosphate, pyromorphite (Pb-phosphate) and zinc phosphate (Gharieb *et al*., 1999; Whitelaw *et al*., 1999; Fomina *et al*., 2004; Pradhan and Sukla, 2006). The significant increase of soluble P_i in MCD medium with incubation time indicated that the REE-phosphates in monazite were dissociating under the effects of fungal-produced acids. The significantly higher amounts of P_i in the monazite-containing MCD medium from the third week onwards confirmed that considerable amounts of REE-phosphates were solubilized.

Pearson correlation analysis revealed the relationship between organic acid production and dissociation of REE-phosphates and provided further evidence for the role that acids played. The very strong correlation between citric acid production and REE implied that there was a synergistic interaction between REE ions and citric acid. The weak relationship between REE and oxalic acid implied that the formation of soluble REE–oxalate complexes was unlikely. Citric acid is not a strong acid with dissociation constants of $K_{a1} = 7.4 \times 10^{-4}$, $K_{a2} = 1.7 \times 10^{-5}$ and $K_{a3} = 5.4 \times 10^{-7}$ (Alkhaldi *et al*., 2010), whereas those of oxalic acid are $K_{a1} = 5.32 \times 10^{-2}$ and $K_{a2} = 1.53 \times 10^{-4}$ at 25 °C (Cruywagen and Heyns, 1983). However, citric acid is endowed with a higher complexing ability as it has three carboxylic acid groups (-COOH) upon which complex formation depends (Bolan *et al*., 1994; Gadd, 1999). Due to this characteristic, citric acid was found to be more effective than other LMWOAs in mobilizing REE from apatite (Ca-phosphate) and monazite (Goyne *et al*., 2010; Brisson *et al*., 2016). A comparative study investigating the bioleaching of uranium from uraninite (UO_2) found that citric acid was more advantageous over oxalic acid with the former achieving a leaching rate at 97% and the latter at 67% (Xu *et al*., 2019). The synergistic behaviour suggested that Ln^{3+} and $(C_6H_5O_7)^{3-}$ may have formed stable complexes since many metals including Cd^{2+}, Cu^{2+}, Fe^{2+}, Fe^{3+}, Ni^{2+}, Pb^{2+} and UO_2^{2+} can form equimolar complexes with the biogenic citrate anion (Francis *et al*., 1992). Calcium can form the well-known calcium–citrate complexes consisting of $CaCit^-_{(aq)}$, $CaHCit_{(aq)}$ and $CaH_2Cit^+_{(aq)}$ (Pak *et al*., 1987). The structure of biogenic REE–citrate complexes appears to be more complex and there is only limited information regarding chemically formed Ce or La complexes. One report showed that LaH_2Cit, LaHCit and LaCit were formed in a 1:1 $LaCl_3$ and citric acid mixture (Barnes and Bristow, 1970). Another study reported that in biological systems, several trivalent lanthanides (La, Nd, Eu, Gd, Tb, Ho and Lu) can form four types of complexes with citric acid in the following manner (Zabiszak *et al*., 2018):

$$Ln^{3+} + HCit \leftrightarrows LnHCit \quad (5)$$

$$Ln^{3+} + Cit \leftrightarrows LnCit \quad (6)$$

$$LnCit + H_2O \leftrightarrows LnCit(OH) \quad (7)$$

$$LnCit(OH) + H_2O \leftrightarrows LnCit(OH)_2 \quad (8)$$

In contrast, most studies suggest that oxalic acid is more effective as a precipitant for many metals even at very low pH (Gharieb *et al*., 1998; Fomina *et al*., 2005b; Wei *et al*., 2013; Brisson *et al*., 2016; Suyamud *et al*., 2020). However, it should not be inferred from the present results that citric acid was more important than oxalic acid in the bioweathering of monazite since the

former was only present in small amount. Studies have shown that fungal-produced oxalic acid is also an effective agent that can form complexes with a wide range of metals such as Al, Cd, Fe, Li and Mn (Strasser *et al*., 1994; Gadd, 1999; Xu *et al*., 2015). In addition, solution chemistry calculations and experimental results revealed that REE can form complexes and be precipitated in leachates with an excessive amount of oxalic acid (Chi and Xu, 1999). Therefore, it is highly likely that in the present study a fraction of REE was also solubilized by *A*. *niger*-produced oxalic acid. The strong positive correlation between P_i and REE concentrations in MCD medium indicated the dissociation of REE-phosphate.

In conclusion, *A*. *niger* was able to colonize high-grade monazite ore and colonization appeared to be enhanced by the presence of essential trace metals in the ore. On monazite surfaces teeth-like patterns were observed, which were indicative of biochemical etching and biomechanical weathering by the mycelia. As time elapsed, biomechanical effects intensified causing aggressive tunnelling and penetration of hyphae into cavities and cracks in the substrate, which subsequently fragmented. Liquid medium experiments suggested that citric acid played a role in the solubilization of REE from monazite while oxalic acid was mainly responsible for solubilization and precipitation of REE into oxalates. Our findings add to the fundamental knowledge regarding direct interactions between fungi and metal-bearing minerals, with implications for REE biogeochemistry as well as new approaches in biohydrometallurgy and biomining technologies.

Experimental procedures

Organism, media and mineral

A wild-type strain of *A*. *niger* (ATCC 1015), routinely maintained on malt extract agar (MEA) (Lab M Limited, Bury, UK) in the dark at 25 °C, was used in the present study. MCD medium consisted of (1^{-1} Milli-Q water): D-glucose 30 g, $NaNO_3$ 2 g, Na_2HPO_4 1 g, $MgSO_4{\cdot}7H_2O$ 0.5 g, KCl 0.5 g, $FeSO_4{\cdot}7H_2O$ 0.01 g and agar No.1 (Lab M Limited) 15 g. The final pH was adjusted to pH 5.5 with sterile 1 M HCl prior to autoclaving for 15 min at 115 °C. MEA was prepared by adding 20 g commercial MEA (Sigma-Aldrich, St Louis, MO, USA) into 1 L Milli-Q water and autoclaving at 115 °C for 15 min. Liquid MCD medium was prepared as above but without addition of agar. The monazite concentrate, which originated from the Gakara rare earth deposit, Burundi, East Africa, was kindly provided by Rainbow Rare Earths Limited (London, UK).

Microcosm experiments

Non-sieved monazite rock particles measuring $\sim 2 \times 3$ mm were used for the investigation of *in situ* colonization and bioweathering by *A*. *niger*. The rock particles were autoclaved for 15 min at 115 °C and dried at 60 °C in an oven for 48 h before being embedded in molten MEA and MCD agar in an equidistant pattern in 90-mm diameter Petri dishes. When solidified, a 0.5-cm-diameter plug of *A*. *niger*, taken from the leading edge of an actively growing colony, was inoculated at the centre of the plate. Plates were incubated at 25 °C in the dark for a total length of 5 weeks. The fungal-colonized monazite was harvested using a scalpel along with the surrounding agar and put in a beaker containing Milli-Q water. The beaker was heated in a microwave oven for 5 min at 900 W until any agar encasing the monazite had completed dissolved. The rock particles were removed from the water using clean tweezers and immediately fixed in 2.5% (vol./vol.) glutaraldehyde-PIPES solution.

Direct interaction in liquid medium

Plugs of *A*. *niger* (0.5 cm diameter), cut from the edge of freshly grown *A*. *niger* colonies for 5 days, were inoculated into pH 5.5 liquid MCD medium at 10 plugs per 100 ml in a 250 ml Erlenmeyer flask, which was shake incubated for 3 days in the dark (125 rpm, 25 °C). After this time, 2 g monazite sand, which had been autoclaved for 15 min at 115 °C and oven-dried at 60 °C, was added into the flask and incubation continued for a total length of 5 weeks. At the end of each week, triplicate aliquots of 1 ml were taken from each sample and used for quantitative analysis of organic acids, soluble P, pH and REE.

Determination of REE and inorganic phosphate (P_i)

Total REE concentration in the liquid medium was measured using the Arsenazo III colorimetric method (Hogendoorn *et al*., 2018). This was achieved by mixing 1 ml of an appropriately diluted sample with 1 ml 0.02% (wt./vol.) Arsenazo III solution (Sigma-Aldrich) and 8 ml pH 2.8 potassium hydrogen phthalate buffer. After colour development, OD_{658nm} was measured using an Ultrospec 2100 pro spectrophotometer (Biochrom, Holliston, MA, USA). REE concentration in the samples was calculated according to a standard curve created using 0, 0.1, 0.2, 0.3, 0.5 and 1.0 mg L^{-1} REE (Ce^{3+}). All samples were measured at least in triplicate.

Determination of P_i concentration in liquid samples was carried out using the vanadate-molybdate method. Analyses were carried out by mixing 1 ml sample or standard P_i solution with 0.25 ml vanadate-molybdate reagent (Sigma-Aldrich) in a plastic cuvette (Sarstedt AG & KG,

Nümbrecht, Germany) and maintaining for 15 min at room temperature for the colour to develop. The OD_{470nm} of the mixture was then measured using an Ultrospec 2100 pro spectrophotometer (Biochrom). P_i concentrations in the samples were calculated according to a standard curve which was prepared by dilution of a stock solution of 8 mM KH_2PO_4 in Milli-Q water to solutions of 100, 300, 500, 800, 1000 and 1200 μM KH_2PO_4. Measurements were carried out at least in triplicate.

Determination of organic acids

Determination of organic acids in appropriately diluted liquid samples was carried out using an UltiMate 3000 high-performance liquid chromatography (HPLC) system (Dionex, San Diego, CA, USA). Standard organic acid solutions were 5, 10, 15 and 20 mM citric acid (Sigma-Aldrich); 1, 2, 3 and 4 mM oxalic acid (Sigma-Aldrich). All samples and standards were filtered through 0.25 μm Minisart syringe filters (Sartorius Stedim Biotech GmbH, Göttingen, Germany) and pipetted into HPLC certified vials (Sigma-Aldrich). The mobile phase was 5 mM H_2SO_4, which was prepared using HPLC LiChropur 98% sulfuric acid (Merck KGaA, Darmstadt, Germany) and degassed by pump-filtration through 0.45 μm Whatman cellulose nitrate membrane filters (GE Healthcare, Buckinghamshire, UK). An Aminex HPX-87H column in connection with a Micro-Guard cation H^+ refill cartridge (Bio-Rad Laboratories, CA, USA) was included in the HPLC system. The parameters for the HPLC system were as follows: flow rate 0.6 ml min^{-1}, column temperature 35 °C, sample injection volume 20 μl and wavelength of the UV detector set at 210 nm. The organic acid separation and detection results were exported as a chromatogram with peak areas automatically integrated by the Chromeleon 6.8 Chromatography Data System Software (Thermo Fisher Scientific, MA, USA) using the default settings. The concentration of organic acids was calculated according to standard curves of peak area versus acid concentration. All measurements were performed in triplicate.

Light microscopy

The monazite rock particles in the colonization experiments were examined using a MOTIC SMZ-168 stereo microscope (Motic Deutschland GmbH, Wetzlar, Germany). The samples were photographed using a ZEISS Axiocam 105 colour digital camera using the ZEN 2 lite software (Carl Zeiss Microscopy, NY, USA).

Fixation and dehydration of samples

The 2.5% (vol./vol.) glutaraldehyde-PIPES solution for fixation of biomass-associated materials was prepared by adding 2.5 ml 25% glutaraldehyde (Sigma-Aldrich) into a volumetric flask and brought up to 100 ml using 5 mM piperazine-*N*,*N*′-bis(2-ethanesulfonic acid) (PIPES buffer), which was then adjusted to pH 6.5 using 1 M NaOH. The biomass-associated samples were immersed in the solution immediately after being harvested from the solid or liquid media. After incubation for at least 24 h at room temperature, the samples were rinsed twice in 5 mM PIPES buffer pH 6.5 (15 min per rinse) to remove residual glutaraldehyde. Ethanol dehydration was then carried out by immersing the samples in ethanol solutions in the following order: 50%, 70%, 80%, 90%, 96% and 100% (vol./vol.) ethanol for 10 min per treatment. Samples were subsequently dehydrated using a liquid CO_2 BAL-TEC CPD 0.30 critical point dryer (BAL-TEC Company, Canonsburg, USA).

EDXA and SEM

The elemental composition of the monazite samples was determined using EDXA. Morphological features of the minerals were examined using SEM. Mineral samples, which were dried in a desiccator for at least 1 week at ambient temperature and critical point dried biomass-associated minerals were mounted on adhesive carbon tape on 25 mm × 5 mm SEM aluminium stubs (Agar Scientific, Essex, UK) before being examined using an EDXA system (Oxford Inca, Abingdon, Oxon, UK) operating in conjunction with a Jeol JSM-7400F field emission scanning electron microscope (JEOL, Tokyo, Japan) at an accelerating voltage of 15 kV for 100 s. Samples for SEM were coated with a layer of 10 nm gold and platinum using a Cressington 208HR sputter coater (Ted Pella, Redding, CA, USA) prior to examination using a field emission scanning electron microscope (Jeol JSM7400F) operating at an accelerating voltage of 5 kV.

Statistical analysis

Data regarding biomass yield, pH, and concentrations of organic acids, solubilized phosphorus and REE were subjected to statistical analysis using R version 4.0.2 (The R Foundation, Vienna, Austria). To compare the significance of difference at $P < 0.05$ between treatments, Tukey's HSD post-hoc test was carried out by executing the glht function based on a fitted analysis of variance model created using the aov function. The pairwise comparison of significance between variables was performed through the independent two-group Student's *t*-test using the t.test function following a Shapiro–Wilk test. Pearson

correlation scatter plots were created using the software package ggpubr version 0.4.0 to analyse correlations between two sets of variables. All test results were based on at least three replicates for each treatment.

Acknowledgements

Xia Kang gratefully acknowledges the receipt of a joint PhD scholarship from the School of Life Sciences, University of Dundee and China Scholarship Council (No. 201606910077). G.M.G. gratefully thanks the Natural Environment Research Council (NE/M010910/1 (TeaSe); NE/M011275/1 (COG^3)) for financial support of the Geomicrobiology Group. The authors also greatly acknowledge Mr. Martin Eales, CEO of Rainbow Rare Earths (London, UK) for kindly providing the monazite sample and Dr. Yongchang Fan (Materials and Photonics Systems Group, University of Dundee) for assistance with scanning electron microscopy and energy-dispersive X-ray spectroscopy.

References

Adeyemi, A.O., and Gadd, G.M. (2005). Fungal degradation of calcium, lead-and silicon-bearing minerals. *Biometals*, **18**, 269–281. https://link.springer.com/content/pdf/10.1007/s10534-005-1539-2.pdf.

Aghaie, E., Pazouki, M., Hosseini, M.R., Ranjbar, M., and Ghavipanjeh, F. (2009) Response surface methodology (RSM) analysis of organic acid production for kaolin beneficiation by *Aspergillus niger*. *Chem Eng J* **147**: 245–251.

Alkhaldi, M.H., Nasr-El-Din, H.A., and Sarma, H.K. (2010) Kinetics of the reaction of citric acid with calcite. *SPE J* **15**: 704–713.

Amiri, F., Mousavi, S.M., Yaghmaei, S., and Barati, M. (2012) Bioleaching kinetics of a spent refinery catalyst using *Aspergillus niger* at optimal conditions. *Biochem Eng J* **67**: 208–217.

Anderson, S.W., Christensen, K., and LaManna, J. (2019) The development of natural resources in outer space. *J Energy Nat Resour Law* **37**: 227–258.

Bahaloo-Horeh, N., and Mousavi, S.M. (2017) Enhanced recovery of valuable metals from spent lithium-ion batteries through optimization of organic acids produced by *Aspergillus niger*. *Waste Manag* **60**: 666–679.

Barmettler, F., Castelberg, C., Fabbri, C., and Brandl, H. (2016) Microbial mobilization of rare earth elements (REE) from mineral solids - a mini review. *AIMS Microbiol* **2**: 190–204.

Barnes, J.C., and Bristow, P.A. (1970) Lanthanum citrate complexes in acid solutions. *J Less-Common Met* **22**: 463–465.

Bennett, J.W. (1998) Mycotechnology: the role of fungi in biotechnology. *J Biotechnol* **66**: 101–107.

Betiku, E., Emeko, H.A., and Solomon, B.O. (2016) Fermentation parameter optimization of microbial oxalic acid production from cashew apple juice. *Heliyon* **2**: e00082.

Bolan, N.S., Naidu, R., Mahimairaja, S., and Baskaran, S. (1994) Influence of low-molecular-weight organic acids on the solubilization of phosphates. *Biol Fert Soils* **18**: 311–319.

Brisson, V.L., Zhuang, W.Q., and Alvarez-Cohen, L. (2016) Bioleaching of rare earth elements from monazite sand. *Biotechnol Bioeng* **113**: 339–348.

Burford, E.P., Fomina, M., and Gadd, G.M. (2003b) Fungal involvement in bioweathering and biotransformation of rocks and minerals. *Miner Mag* **67**: 1127–1155.

Burford, E.P., Kierans, M., and Gadd, G.M. (2003a) Geomycology: fungi in mineral substrata. *Mycologist* **17**: 98–107.

Ceci, A., Kierans, M., Hillier, S., Persiani, A.M., and Gadd, G.M. (2015b) Fungal bioweathering of mimetite and a general geomycological model for lead apatite mineral biotransformations. *Appl Environ Microbiol* **81**: 4955–4964.

Ceci, A., Rhee, Y.J., Kierans, M., Hillier, S., Pendlowski, H., Gray, N., *et al*. (2015a) Transformation of vanadinite [$Pb_5(VO_4)_3Cl$] by fungi. *Environ Microbiol* **17**: 2018–2034.

Chi, R.A., and Xu, Z.G. (1999) A solution chemistry approach to the study of rare earth element precipitation by oxalic acid. *Metall Mater Trans B* **30**: 189–195.

Cockell, C.S., Santomartino, R., Finster, K., Waajen, A.C., Eades, L.J., Moeller, R., *et al*. (2020) Space station biomining experiment demonstrates rare earth element extraction in microgravity and Mars gravity. *Nat Commun* **11**: 552.

Cruywagen, J.J., and Heyns, J.B.B. (1983) Determination of the dissociation constants of oxalic acid and the ultraviolet spectra of the oxalate species in 3M perchlorate medium. *Talanta* **30**: 197–200.

de la Torre, M.A., Gomez-Alarcon, G., Vizcaino, C., and Garcia, M.T. (1992) Biochemical mechanisms of stone alteration carried out by filamentous fungi living in monuments. *Biogeochemistry* **19**: 129–147.

Dickson, A.G., and Riley, J.P. (1979) The estimation of acid dissociation constants in seawater media from potentionmetric titrations with strong base. I. the ionic product of water-K_w. *Mar Chem* **7**: 89–99.

Dixon-Hardy, J.E., Karamushka, V.I., Gruzina, T.G., Nikovska, G.N., Sayer, J.A., and Gadd, G.M. (1998) Influence of the carbon, nitrogen and phosphorus source on the solubilization of insoluble metal compounds by *Aspergillus niger*. *Mycol Res* **102**: 1050–1054.

Faraji, F., Golmohammadzadeh, R., Rashchi, F., and Alimardani, N. (2018) Fungal bioleaching of WPCBs using *Aspergillus niger*: observation, optimization and kinetics. *J Environ Manage* **217**: 775–787.

Ferrier, J., Yang, Y., Csetenyi, L., and Gadd, G.M. (2019) Colonization, penetration and transformation of manganese oxide nodules by *Aspergillus niger*. *Environ Microbiol* **21**: 1821–1832.

Fomina, M., Alexander, I.J., Hillier, S., and Gadd, G.M. (2004) Zinc phosphate and pyromorphite solubilization by soil plant-symbiotic fungi. *Geomicrobiol J* **21**: 351–366.

Fomina, M., Burford, E.P., Hillier, S., Kierans, M., and Gadd, G.M. (2010) Rock-building fungi. *Geomicrobiol J* **27**: 624–629.

Fomina, M., Charnock, J.M., Hillier, S., Alexander, I.J., and Gadd, G.M. (2006) Zinc phosphate transformations by the *Paxillus involutus*/pine ectomycorrhizal association. *Microbial Ecol* **52**: 322–333.

Fomina, M., Hillier, S., Charnock, J.M., Melville, K., Alexander, I.J., and Gadd, G.M. (2005b) Role of oxalic acid over-excretion in toxic metal mineral transformations by *Beauveria caledonica*. *Appl Environ Microbiol* **71**: 371–381.

Fomina, M.A., Alexander, I.J., Colpaert, J.V., and Gadd, G.M. (2005a) Solubilization of toxic metal minerals and metal tolerance of mycorrhizal fungi. *Soil Biol Biochem* **37**: 851–866.

Francis, A.J., Dodge, C.J., and Gillow, J.B. (1992) Biodegradation of metal citrate complexes and implications for toxic-metal mobility. *Nature* **356**: 140–142.

Fuhr, M.J., Schubert, M., Stührk, C., Schwarze, F.W., and Herrmann, H.J. (2013) Penetration capacity of the wood-decay fungus *Physisporinus vitreus*. *Complex Adapt Syst Model* **1**: 6.

Gadd, G.M. (1999) Fungal production of citric and oxalic acid: importance in metal speciation, physiology and biogeochemical processes. *Adv Microb Physiol* **41**: 47–92.

Gadd, G.M. (2007) Geomycology: biogeochemical transformations of rocks, minerals, metals and radionuclides by fungi, bioweathering and bioremediation. *Mycol Res* **111**: 3–49.

Gadd, G.M. (2010) Metals, minerals and microbes: geomicrobiology and bioremediation. *Microbiol* **156**: 609–643.

Gadd, G.M. (2017a) Fungi, rocks, and minerals. *Elements* **13**: 171–176.

Gadd, G.M. (2017b) The geomycology of elemental cycling and transformations in the environment. *Microbiol Spectr* **5**: 1–16.

Gadd, G.M. (2017c) Geomicrobiology of the built environment. *Nat Microbiol* **2**: 16275.

Gadd, G.M., Bahri-Esfahani, J., Li, Q., Rhee, Y.J., Wei, Z., Fomina, M., and Liang, X. (2014) Oxalate production by fungi: significance in geomycology, biodeterioration and bioremediation. *Fungal Biol Rev* **28**: 36–55.

Gharieb, M.M., and Gadd, G.M. (1999) Influence of nitrogen source on the solubilization of natural gypsum ($CaSO_4{\cdot}2H_2O$) and the formation of calcium oxalate by different oxalic and citric acid-producing fungi. *Mycol Res* **103**: 473–481.

Gharieb, M.M., Kierans, M., and Gadd, G.M. (1999) Transformation and tolerance of tellurite by filamentous fungi: accumulation, reduction, and volatilization. *Mycol Res* **103**: 299–305.

Gharieb, M.M., Sayer, J.A., and Gadd, G.M. (1998) Solubilization of natural gypsum ($CaSO_4{\cdot}2H_2O$) and the formation of calcium oxalate by *Aspergillus niger* and *Serpula himantioides*. *Mycol Res* **102**: 825–830.

Gleeson, D.B., Clipson, N., Melville, K., Gadd, G.M., and McDermott, F.P. (2005) Characterization of fungal community structure on a weathered pegmatitic granite. *Microb Ecol* **50**: 360–368.

Goodenough, K.M., Schilling, J., Jonsson, E., Kalvig, P., Charles, N., and Tuduri, J. (2016) Europe's rare earth element resource potential: an overview of REE metallogenetic provinces and their geodynamic setting. *Ore Geol Rev* **72**: 838–856.

Goyne, K.W., Brantley, S.L., and Chorover, J. (2010) Rare earth element release from phosphate minerals in the presence of organic acids. *Chem Geol* **278**: 1–14.

Graedel, T.E., Harper, E.M., Nassar, N.T., Nuss, P., and Reck, B.K. (2015) Criticality of metals and metalloids. *Proc Natl Acad Sci U S A* **112**: 4257–4262.

Haque, N., Hughes, A., Lim, S., and Vernon, C. (2014) Rare earth elements: overview of mining, mineralogy, uses, sustainability and environmental impact. *Resources* **3**: 614–635.

Hassanien, W.A.G., Desouky, O.A.N., and Hussien, S.S.E. (2014) Bioleaching of some rare earth elements from Egyptian monazite using *Aspergillus ficuum* and *Pseudomonas aeruginosa*. *Walailak J Sci Technol* **11**: 809–823.

Hein, J. (2016) Manganese nodules. In *Encyclopedia of Marine Geosciences*, Harff, J., Meschede, M., Petersen, S., and Thiede, J. (eds). Dordrecht, the Netherlands: Springer, pp. 408–412.

Hein, J.R., Mizell, K., Koschinsky, A., and Conrad, T.A. (2013) Deep-ocean mineral deposits as a source of critical metals for high- and green-technology applications: comparison with land-based resources. *Ore Geol Rev* **51**: 1–14.

Hirsch, P., Eckhardt, F.E.W., and Palmer, R.J., Jr. (1995) Fungi active in weathering of rock and stone monuments. *Can J Bot* **73**: 1384–1390.

Hoffland, E., Kuyper, T.W., Wallander, H., Plassard, C., Gorbushina, A.A., Haselwandter, K., *et al*. (2004) The role of fungi in weathering. *Front Ecol Environ* **2**: 258–264.

Hogendoorn, C, Roszczenko-Jasińska, P, Martinez-Gomez, N.C, de Graaff, J, Grassl, P, and Pol, A (2018). A facile Arsenazo III based assay for monitoring rare earth element depletion from cultivation media of methanotrophic and methylotrophic bacteria. *Appl Environ Microbiol*, **84**, e02887–17. https://aem.asm.org/content/84/8/e02887-17.short.

Hossain, M., Brooks, J.D., and Maddox, I.S. (1984) The effect of the sugar source on citric acid production by *Aspergillus niger*. *Appl Microbiol Biot* **19**: 393–397.

Humphries, M. (2012) *Rare Earth Elements: The Global Supply Chain*. Washington, DC: U.S. Congressional Research Service.

Jacobs, H., Boswell, G.P., Ritz, K., Davidson, F.A., and Gadd, G.M. (2002a) Solubilization of metal phosphates by *Rhizoctonia solani*. *Mycol Res* **106**: 1468–1479.

Jacobs, H., Boswell, G.P., Ritz, K., Davidson, F.A., and Gadd, G.M. (2002b) Solubilization of calcium phosphate as a consequence of carbon translocation by *Rhizoctonia solani*. *FEMS Microbiol Ecol* **40**: 65–71.

Jan, D.C.H., Jones, S.J., Emery, A.N., and Al-Rubeai, M. (1994) Peptone, a low-cost growth-promoting nutrient for intensive animal cell culture. *Cytotechnology* **16**: 17–26.

Jiang, C. (1996) Thermodynamics of aqueous phosphoric acid solution at 25°C. *Chem Eng Sci* **51**: 689–693.

Johnson, D.B. (2014) Biomining - biotechnologies for extracting and recovering metals from ores and waste materials. *Curr Opinion Biotechnol* **30**: 24–31.

Johnson, D.B. (2018) The evolution, current status and future prospects of using biotechnologies in the mineral extraction and metal recovery sectors. *Minerals* **8**: 343.

Jongmans, A.G., van Breemen, N., Lundström, U., van Hees, P.A.W., Finlay, R.D., Srinivasan, M., *et al*. (1997) Rock-eating fungi. *Nature* **389**: 682–683.

Kang, X., Csetenyi, L., and Gadd, G.M. (2019) Biotransformation of lanthanum by *Aspergillus Niger*. *Appl Microbiol Biot* **103**: 981–993.

Kang, X., Csetenyi, L., and Gadd, G.M. (2020) Monazite transformation into Ce- and La-containing oxalates by *Aspergillus niger*. *Environ Microbiol* **22**: 1635–1648.

Kirtzel, J., Ueberschaar, N., Deckert-Gaudig, T., Krause, K., Deckert, V., Gadd, G.M., and Kothe, E. (2020) Organic acids, siderophores, enzymes and mechanical pressure for black slate bioweathering with the basidiomycete *Schizophyllum commune*. *Environ Microbiol* **22**: 1535–1546.

Kuhn, T., Wegorzewski, C., Rühlemann, C., and Vink, A. (2017) Composition, formation, and occurrence of polymetallic nodules. In *Deep-Sea Mining: Resource Potential, Technical and Environmental Considerations*, Sharma, R. (ed). NY, USA: Springer International Publishing, pp. 23–63.

Kumari, A., Panda, R., Jha, M.K., Kumar, J.R., and Lee, J.Y. (2015) Process development to recover rare earth metals from monazite mineral: a review. *Miner Eng* **79**: 102–115.

Landeweert, R., Hoffland, E., Finlay, R.D., Kuyper, T.W., and van Breemen, N. (2001) Linking plants to rocks: ectomycorrhizal fungi mobilize nutrients from minerals. *Trends Ecol Evol* **16**: 248–254.

Liang, X., and Gadd, G.M. (2017) Metal and metalloid biorecovery using fungi. *J Microbial Biotechnol* **10**: 1199–1205.

Liang, X., Kierans, M., Ceci, A., Hillier, S., and Gadd, G.M. (2016) Phosphatase-mediated bioprecipitation of lead by soil fungi. *Environ Microbiol* **18**: 219–231.

Ma, W., Wu, F., Tian, T., He, D., Zhang, Q., Gu, J.-D., *et al*. (2020) Fungal diversity and its contribution to the biodeterioration of mural paintings in two 1700-year-old tombs of China. *Int Biodeter Biodegr* **152**: 104972.

Magnuson, J.K., and Lasure, L.L. (2004) Organic acid production by filamentous fungi. In *Advances in Fungal Biotechnology for Industry, Agriculture, and Medicine*, Tkacz, J.S., and Lange, L. (eds). Boston: Springer, pp. 307–340.

Massari, S., and Ruberti, M. (2013) Rare earth elements as critical raw materials: focus on international markets and future strategies. *Resour Policy* **38**: 36–43.

McLeod, C.L., and Krekeler, M.P.S. (2017) Sources of extraterrestrial rare earth elements: to the moon and beyond. *Resources* **6**: 40.

Mendes, G.de O, Murta, H.M, Valadares, R.V, da Silveira, W.B, da Silva, I.R, and Costa, M.D (2020). Oxalic acid is more efficient than sulfuric acid for rock phosphate solubilization. *Miner Eng*, **155**, 106458. https://www.sciencedirect.com/science/article/abs/pii/S0892687520302788#!.

Mergelov, N., Mueller, C.W., Prater, I., Shorkunov, I., Dolgikh, A., Zazovskaya, E., *et al*. (2018) Alteration of rocks by endolithic organisms is one of the pathways for the beginning of soils on Earth. *Sci Rep-UK* **8**: 1–15.

Mottershead, D., Gorbushina, A., Lucas, G., and Wright, J. (2003) The influence of marine salts, aspect and microbes in the weathering of sandstone in two historic structures. *Build Environ* **38**: 1193–1204.

Padmavathi, T. (2015) Optimization of phosphate solubilization by *Aspergillus niger* using plackett-burman and response surface methodology. *J Soil Sci Plant Nutr* **15**: 781–793.

Paik, J., Low, N.H., and Ingledew, W.M. (1991) Malt extract: relationship of chemical composition to fermentability. *J Am Soc Brew Chem* **49**: 8–13.

Pak, C.Y.C., Harvey, J.A., and Hsu, M.C. (1987) Enhanced calcium bioavailability from a solubilized form of calcium citrate. *J Clin Endocrinol Metab* **65**: 801–805.

Pradhan, N., and Sukla, L.B. (2006) Solubilization of inorganic phosphates by fungi isolated from agriculture soil. *Afr J Biotechnol* **5**: 850–854.

Ruijter, G.J.G., van de Vondervoort, P.J.I., and Visser, J. (1999) Oxalic acid production by *Aspergillus niger*: an oxalate-non-producing mutant produces citric acid at pH 5 and in the presence of manganese. *Microbiology* **145**: 2569–2576.

Saber, W.I.A., Ghanem, K.M., and El-Hersh, M.S. (2009). Rock phosphate solubilization by two isolates of Aspergillus niger and Penicillium sp. and their promotion to mung bean plants. *Res J Microbiol*, **4**, 235–250. https://www.cabdirect.org/cabdirect/abstract/20093342688.

Schneider, K.D., van Straaten, P., Mira de Orduña, R., Glasauer, S., Trevors, J., Fallow, D., *et al*. (2010) Comparing phosphorus mobilization strategies using *Aspergillus niger* for the mineral dissolution of three phosphate rocks. *J Appl Microbiol* **108**: 366–374.

Skinner, B.J. (1979) Earth resources. *Proc Natl Acad Sci U S A* **76**: 4212–4217.

Staley, J.T., Palmer, F., and Adams, J.B. (1982) Microcolonial fungi: common inhabitants on desert rocks? *Science* **215**: 1093–1095.

Strasser, H., Burgstaller, W., and Schinner, F. (1994) High-yield production of oxalic acid for metal leaching processes by *Aspergillus niger*. *FEMS Microbiol Lett* **119**: 365–370.

Sturm, E.V., Frank-Kamenetskaya, O., Vlasov, D., Zelenskaya, M., Sazanova, K., Rusakov, A., *et al*. (2015) Crystallization of calcium oxalate hydrates by interaction of calcite marble with fungus *Aspergillus niger*. *Am Mineral* **100**: 2559–2565.

Suyamud, B., Ferrier, J., Csetenyi, L., Inthorn, D., and Gadd, G.M. (2020) Biotransformation of struvite by *Aspergillus niger*: phosphate release and magnesium biomineralization as glushinskite. *Environ Microbiol* **22**: 1588–1602.

Upton, D.J., McQueen-Mason, S.J., and Wood, A.J. (2017) An accurate description of *Aspergillus niger* organic acid batch fermentation through dynamic metabolic modelling. *Biotechnol Biofuels* **10**: 258.

Uroz, S., Calvaruso, C., Turpault, M.-P., and Frey-Klett, P. (2009) Mineral weathering by bacteria: ecology, actors and mechanisms. *Trends Microbiol* **17**: 378–387.

van Schöll, L., Kuyper, T.W., Smits, M.M., Landeweert, R., Hoffland, E., and van Breemen, N. (2008) Rock-eating mycorrhizas: their role in plant nutrition and biogeochemical cycles. *Plant Soil* **303**: 35–47.

Wall, F., Rollat, A., and Pell, R.S. (2017) Responsible sourcing of critical metals. *Elements* **13**: 313–318.

Wei, Z., Kierans, M., and Gadd, G.M. (2012) A model sheet mineral system to study fungal bioweathering of mica. *Geomicrobiol J* **29**: 323–331.

Wei, Z., Liang, X., Pendlowski, H., Hillier, S., Suntornvongsagul, K., Sihanonth, P., and Gadd, G.M. (2013) Fungal biotransformation of zinc silicate and sulfide mineral ores. *Environ Microbiol* **15**: 2173–2186.

Whitelaw, M.A. (1999) Growth promotion of plants inoculated with phosphate solubilizing fungi. *Adv Agron* **69**: 99–151.

Whitelaw, M.A., Harden, T.J., and Helyar, K.R. (1999) Phosphate solubilisation in solution culture by the soil fungus *Penicillium radicum*. *Soil Biol Biochem* **31**: 655–665.

Wollenzien, U., de Hoog, G., Krumbein, W., and Urzi, C. (1995) On the isolation of microcolonial fungi occurring on and in marble and other calcareous rocks. *Sci Total Environ* **167**: 287–294.

Xu, L., Yang, H., Liu, Y., and Zhou, Y. (2019) Uranium leaching using citric acid and oxalic acid. *J Radioanal Nucl Ch* **321**: 815–822.

Xu, P., Leng, Y., Zeng, G., Huang, D., Lai, C., Zhao, M., *et al*. (2015) Cadmium induced oxalic acid secretion and its role in metal uptake and detoxification mechanisms in *Phanerochaete chrysosporium*. *Appl Microbiol Biot* **99**: 435–443.

Yang, Y., Ferrier, J., Csetenyi, L., and Gadd, G.M. (2019) Direct and indirect bioleaching of cobalt from low grade laterite and pyritic ores by *Aspergillus niger*. *Geomicrobiol J* **36**: 940–949.

Zabiszak, M., Nowak, M., Taras-Goslinska, K., Kaczmarek, M.T., Hnatejko, Z., and Jastrzab, R. (2018) Carboxyl groups of citric acid in the process of complex formation with bivalent and trivalent metal ions in biological systems. *J Inorg Biochem* **182**: 37–47.

Zhao, J., Csetenyi, L., and Gadd, G.M. (2020) Biocorrosion of copper metal by *Aspergillus niger*. *Int Biodeter Biodegr* **154**: 105081.

Zhuang, W.-Q., Fitts, J.P., Ajo-Franklin, C.M., Maes, S., Alvarez-Cohen, L., and Hennebel, T. (2015) Recovery of critical metals using biometallurgy. *Curr Opin Biotechnol* **33**: 327–335.